

Abstract

This study explores an approach that simultaneously estimates Antarctic mass balance and glacial isostatic adjustment (GIA) through the combination of satellite gravity and altimetry data sets. The results improve upon previous efforts by incorporating reprocessed data sets over a longer period of time, and now include a firn densification model to account for firn compaction and surface processes. A range of different GRACE gravity models were evaluated, as well as a new ICESat surface height trend map computed using an overlapping footprint approach. When the GIA models created from the combination approach were compared to in-situ GPS ground station displacements, the vertical rates estimated showed consistently better agreement than existing GIA models. In addition, the new empirically derived GIA rates suggest the presence of strong uplift in the Amundsen Sea and Philippi/Denman sectors, as well as subsidence in large parts of East Antarctica. The total GIA mass change estimates for the entire Antarctic ice sheet ranged from 53 to 100 Gt yr⁻¹, depending on the GRACE solution used, and with an estimated uncertainty of ± 40 Gt yr⁻¹. Over the time frame February 2003–October 2009, the corresponding ice mass change showed an average value of -100 ± 44 Gt yr⁻¹ (EA: 5 ± 38 , WA: -105 ± 22), consistent with other recent estimates in the literature, with the mass loss mostly concentrated in West Antarctica. The refined approach presented in this study shows the contribution that such data combinations can make towards improving estimates of present day GIA and ice mass change, particularly with respect to determining more reliable uncertainties.

1 Introduction

Over the past decade, there has been general consensus within the glaciological and geodesy communities that the ice sheet of Antarctica is currently experiencing a significant loss in ice mass, on the order of tens to hundreds of gigatons (1 Gt = 10^{12} kg) per year (Chen et al., 2006; Rignot et al., 2008; Horwath and Dietrich, 2009; Jacob

TCD

7, 3497–3541, 2013

Estimation of present-day Antarctic GIA and ice mass change

B. C. Gunter et al.

Title Page

Abstract

Introduction

Conclusions

References

Tables

Figures

⏪

⏩

◀

▶

Back

Close

Full Screen / Esc

Printer-friendly Version

Interactive Discussion



Estimation of present-day Antarctic GIA and ice mass change

B. C. Gunter et al.

Title Page

Abstract

Introduction

Conclusions

References

Tables

Figures

⏪

⏩

◀

▶

Back

Close

Full Screen / Esc

Printer-friendly Version

Interactive Discussion

because the large density contrast between rock and ice make the altimetry products much more sensitive to the volume changes associated with ice mass changes, while the gravity products are much more sensitive to the mass changes associated with GIA. For example, a 1 cm uplift due to GIA would be barely detectable by satellite altimetry, but the corresponding (large) mass change from this small uplift would be clearly observable from GRACE. Previous studies have demonstrated the feasibility of this approach (Wahr et al., 2000; Velicogna and Wahr, 2002), with the first real-data combination produced by Riva et al. (2009). As a joint estimation problem, GIA and ice mass change trends are simultaneously computed, creating a self-consistent set of estimates. In addition, as a data-driven approach, the errors of the input data sets can be used to generate realistic and spatially varying uncertainties of the resulting GIA and mass change estimates through standard error propagation techniques. In the time since the first real-data combination was achieved, several major improvements to the methodology and data sets have taken place, resulting in new estimates of Antarctic GIA and ice sheet mass balance that this paper seeks to highlight.

New contributions of this study include the use of updated data from GRACE and the Ice Cloud and land Elevation Satellite (ICESat) mission, which have both recently undergone a complete reprocessing that has noticeably improved the data quality compared to previous releases. For the GRACE data, a range of both unconstrained and regularized solutions are evaluated to better categorize the impact that different processing strategies can have on the results. The ICESat data was processed using a recently developed technique involving the use of overlapping footprints (OFPs). The approach was first developed by Slobbe et al. (2008) for a study of the Greenland ice sheet, but has not been applied previously to Antarctica. The OFP approach was expanded and improved for this study, and made use of the latest release of ICESat data (R633). The OFP method has many benefits over standard repeat-track and cross-over techniques, and is particularly well-suited for Antarctica due to the high density of laser shots available. The technique also allows for the independent determination of

3.1 Gravimetry

The GRACE mission has collected data on the time-variable nature of Earth's gravity field since its launch in March 2002. A number of research centers produce monthly gravity field models, using different processing methodologies. A range of gravity models are examined in this study, including those generated by the University of Texas at Austin Center for Space Research (CSR), the GeoForschungsZentrum (GFZ), and Delft University of Technology (TUD). Both RL04 and RL05 solutions were evaluated when available, as well as regularized solutions using various techniques. Degree one coefficients were added to all solutions using values generated from the approach of Swenson et al. (2008) (using RL05 GRACE data), and the $C_{2,0}$ harmonics were replaced with those derived from satellite laser ranging (Cheng and Tapley, 2004). For the RL04 models, the secular trends that are removed from select zonal coefficients were restored, as these rates are believed to mostly represent the effects of GIA.

For all solutions except the Delft Mass Transport (DMT-1b) models produced at TUD (Liu et al., 2010), which use a specialized method for the trend estimation (Siemes et al., 2013), a linear trend was estimated for each harmonic coefficient across the entire time series of monthly models (again, covering only the time period from February 2003 to October 2009). The trend was co-estimated with a bias, annual periodic, and tidal S2 (161 day) periodic terms. Earlier studies (Seo et al., 2008) indicated that additional aliasing may occur at other tidal frequencies, e.g., K2 (1362.7 days); however, an investigation into these showed that only S2 showed a noticeable influence on the long-term trends over Antarctica, particularly for the newer RL05 solutions. Evidence for this is provided in Fig. 1, which shows the amplitude of the estimated K2 periodic signal in units of equivalent water height (EWH) computed from both a representative GRACE solution (CSR RL04 DDK3 in this case) and the 330 km Gaussian smoothed surface mass balance (SMB) estimates from the RACMO2 climate model (see Sect. 3.3). The fact that the majority of the areas with larger amplitudes in the GRACE solution (Fig. 1a) are spatially correlated with those seen in the SMB esti-

Estimation of present-day Antarctic GIA and ice mass change

B. C. Gunter et al.

Title Page

Abstract

Introduction

Conclusions

References

Tables

Figures



Back

Close

Full Screen / Esc

Printer-friendly Version

Interactive Discussion



mates (Fig. 1b), suggests that the signal seen in the GRACE data is genuine mass variability at this frequency.

For the unconstrained CSR and GFZ solutions, the estimated long-term trend was then de-stripped using an approach similar to that outlined by Swenson and Wahr (2006), but with the filtering parameters described by Chambers and Bonin (2012). Even though these parameters were created with ocean applications in mind, the choice of polynomial degree (5th order for RL04, 4th order for RL05) and starting degree and order (12 for RL04, 15 for RL05) were found to perform better than other alternative parameters tested, and were therefore used for this study. No de-stripping was applied to any of the regularized solutions.

Several sets of regularized solutions were included in the analysis, to examine the potential impact that different spatial filtering techniques may have on the final results. This included the Wiener-type filter described by Kusche (2007), which was applied to the RL04 (DDK3) and RL05 (DDK5) solutions for both the CSR and GFZ. A recently developed set of filtered solutions developed by Save et al. (2012), utilizing an L-curve method with Tikhonov regularization, were also evaluated (named here “CSR Reg”). Finally, for the DMT1-b solutions, the anisotropic filtering method developed by Klees et al. (2008) is applied after the long-term coefficient trend is estimated (along with bias, annual, and S2 terms).

Not all solutions are generated to the same spherical harmonic degree and order, and truncating them to the lowest common resolution, e.g., 60×60 , can noticeably degrade their quality. Therefore, most solutions were left in their native resolution when possible, as indicated in Table 2. For the GFZ unconstrained solutions, however, leaving them at their original resolution resulted in the presence of a significant amount of noise in the trends, requiring a small degree of additional Gaussian smoothing after the trend fitting and de-stripping process. The amount of Gaussian smoothing for these unconstrained GFZ solutions was kept at a minimum in an effort to maximize the signal content in the solutions, and was approximately 200 km.

Estimation of present-day Antarctic GIA and ice mass change

B. C. Gunter et al.

Title Page	
Abstract	Introduction
Conclusions	References
Tables	Figures
⏪	⏩
◀	▶
Back	Close
Full Screen / Esc	
Printer-friendly Version	
Interactive Discussion	

Discussion Paper | Discussion Paper | Discussion Paper | Discussion Paper | Discussion Paper



In total, 10 different GRACE solutions were evaluated, with the geographical plots for a representative selection of these cases shown in Fig. 2. The plots for all 10 solutions can be found in Fig. S1 of the Supplement. As can be seen, the trends for nearly all solutions are quite similar; however, some variations can be seen in terms of magnitude and resolution of finer features. As will be seen later, these variations will have an important influence of the outcome of the estimated GIA and ice mass change values from the data combinations.

3.2 Altimetry

The ICESat mission was the first Earth-orbiting laser altimeter and, while no longer operational, it was able to collect valuable information on the long-term surface height change of Antarctica over a period which directly coincides with when the gravity data from GRACE was collected. The surface height change trends used for this study were computed using the latest release of ICESat data (R633), and were computed using an approach involving overlapping footprints (OFPs), similar to that described by Slobbe et al. (2008) for Greenland. This is the first time the OFP approach has been applied to Antarctica. The technique is well suited for observing long term trends at a high spatial resolution, since the co-location of the laser shots used in the height change estimates do not rely on interpolation and/or surface approximations inherent in other techniques, such as cross-over and repeat-track analysis. The technique is particularly useful for height change studies in Antarctica due to the high density of laser shots from the near-polar orbit of ICESat. The data processing uses a set of editing criteria to remove outliers, and estimates a custom set of inter-campaign biases, the details of which are outlined below.

3.2.1 Overlapping footprint approach

The basic principle of the OFP approach is illustrated in Fig. 3a, where an overlapping footprint pair is defined as any two individual ICESat laser shots whose ground foot-

Estimation of present-day Antarctic GIA and ice mass change

B. C. Gunter et al.

Title Page

Abstract

Introduction

Conclusions

References

Tables

Figures



Back

Close

Full Screen / Esc

Printer-friendly Version

Interactive Discussion



computed from individual OFP/NN pairs greater than 12 m yr^{-1} were excluded, as this is assumed larger than most known glacial thinning or ablation processes. A linear trend in time (without annual terms) was fit across all (dh , dt) pairs satisfying the editing criteria within $20 \text{ km} \times 20 \text{ km}$ area blocks, with the uncertainties determined by scaling the formal error from the least squares regression by the estimated variance of unit weight (EVUW) computed from the post-fit residuals (Urban et al., 2013). This EVUW scaling also helps to account for errors due to any seasonal variations that might be present. The estimated dh/dt values from this process are shown in Fig. 4a, with the corresponding uncertainties in Fig. 4b. When integrated only over the grounded ice sheet, using the boundaries defined by Zwally et al. (2012), the total volume change is approximately $-109 \pm 68 \text{ km}^3 \text{ yr}^{-1}$. Most of the uncertainty is located in the Antarctic Peninsula and Transantarctic Mountains, and is caused by both a combination of poor sampling and steep topography.

3.2.2 Estimation of campaign biases

The ICESat laser shots are known to have a systematic bias in them that can introduce cm-level errors if neglected (Gunter et al., 2009). To minimize the effect of these campaign-specific biases, an approach to estimate their magnitude was adopted using a low-precipitation zone (LPZ) in East Antarctica, in the same line as Gunter et al. (2010) and Riva et al. (2009). The rationale is that East Antarctica is one of the driest places on Earth, and has relatively flat topography, so very little surface height change is expected to take place in this region. The exact region used to estimate the campaign biases is shown in Fig. 5, and was derived using output from the regional climate model to be discussed in Sect. 3.3. In particular, the region corresponds to an area that is estimated to have less than $21.9 \text{ mm EWH yr}^{-1}$ of average yearly solid precipitative flux, a value chosen by trial-and-error to create a continuous low-precipitation zone that is sufficiently isolated from areas of steep topography.

Estimation of present-day Antarctic GIA and ice mass change

B. C. Gunter et al.

Title Page

Abstract

Introduction

Conclusions

References

Tables

Figures

⏪

⏩

◀

▶

Back

Close

Full Screen / Esc

Printer-friendly Version

Interactive Discussion



bias offset with respect to the mid-point of the ICESat mission lifetime. The estimated biases were removed from the individual laser shots involved in the height change calculation for each OFP, i.e., before the trend-fitting by blocked area discussed in the previous section.

3.3 Climate data

In order to separate the deformation caused by surface processes (ice, firn) from those of the solid-earth (GIA), both the volume and mass change of the ice sheet needs to be known. There are many complex processes at work that complicate the determination of these quantities, including regional variations in temperature, accumulation, and firn compaction. To account for these, a firn densification model (FDM) developed by Ligtenberg et al. (2011) is used that is forced at the surface with realistic 6 hourly climate output from the regional atmospheric climate model RACMO2 produced by Lenaerts et al. (2012). This FDM model accounts for compaction of the firn over time, and is used in conjunction with the time-varying estimates of the total SMB from RACMO2 to estimate the mass change of the firn layer. Figure 7 shows the total surface height rate, and associated uncertainties, as derived from the FDM model over the study period. It is important to note that the FDM of Fig. 7b only represents the surface height changes of the firn, and does not reflect changes due to either the solid earth or ice dynamics. Furthermore, the mass change of the firn over time, \dot{m}_{firn} , is derived from the SMB, which is a separate product generated from RACMO2, although both the FDM and SMB estimates are inherently linked.

Two basic assumptions were made to account for height differences that were found to exist between the altimetry measurements and the FDM. First, the uncertainties of the height estimates derived from the ICESat and FDM data sets were defined over each grid cell as

$$\sigma_h = \sqrt{\sigma_{\text{ICESat}}^2 + \sigma_{\text{FDM}}^2}, \quad (2)$$

Estimation of present-day Antarctic GIA and ice mass change

B. C. Gunter et al.

Title Page

Abstract

Introduction

Conclusions

References

Tables

Figures

⏪

⏩

◀

▶

Back

Close

Full Screen / Esc

Printer-friendly Version

Interactive Discussion



Estimation of present-day Antarctic GIA and ice mass change

B. C. Gunter et al.

Title Page

Abstract

Introduction

Conclusions

References

Tables

Figures

⏪

⏩

◀

▶

Back

Close

Full Screen / Esc

Printer-friendly Version

Interactive Discussion



using the standard deviations shown in Figs. 4 and 7. In order to convert the volume changes derived from the ICESat data into mass, the density of the volume change needs to be known. Because RACMO2 only models firn processes, any negative differences between the ICESat and FDM surfaces that was greater than $2\sigma_h$ for any given grid cell were assumed to be the result of ice dynamics (glacier thinning), and the density assigned to this volume loss was that of ice (917 kg m^{-3}). Similarly, any positive height differences beyond the $2\sigma_h$ level were attributed to an underestimation of SMB by RACMO2, and given a density closer to that of snow using a static density profile similar to that of Kaspers et al. (2004). The justification for the densities assigned to positive height differences is shown in Fig. 8. This plot shows the derived density (Fig. 8c) computed from those regions where the (GRACE – SMB) differences were greater than $20\text{ kg m}^{-2}\text{ yr}^{-1}$, and the (ICESat – FDM) were greater than 6 cm yr^{-1} . The resulting densities in those areas are predominantly in the $350\text{--}600\text{ kg m}^{-3}$ range, with a mean value of 396 kg m^{-3} , suggesting that the use of snow densities for these positive height anomalies is reasonable. The only exception to the rules of positive or negative height differences was for the region of the Kamb Ice Stream in West Antarctica, where no ice discharge takes place, and the positive height change is assumed to be a build-up of ice (glacier thickening) with a density of 917 kg m^{-3} . If the height differences between ICESat and the FDM fell within the $2\sigma_h$, the height measurements were considered to be within the uncertainty of the data sets, and the volume/mass of the difference was neglected. It is important to note that these assumptions only deal with potential residual signal observed between ICESat and the FDM. The majority of the surface mass changes come directly from the SMB estimates (i.e., \dot{m}_{firn}) derived from RACMO2. As such, the utilization of the SMB and FDM in the combination approach required a modification of Eq. (1),

$$\dot{h}_{\text{rock}} = \frac{\dot{m}_{\text{GRACE}} - [(\dot{h}_{\text{ICESat}} - \dot{h}_{\text{firn}}) \cdot \rho_{\alpha} + \dot{m}_{\text{firn}}]}{\rho_{\text{rock}} - \rho_{\alpha}} \quad (3)$$

Following a similar approach as Whitehouse et al. (2012), comparisons with the GPS data were done by computing the weighted root-mean-square of the residuals (WRMS) between the vertical empirical or modelled rates and those observed from the GPS stations (i),

$$WRMS = \sqrt{\frac{\sum w_i \cdot (\dot{h}_{GIA} - \dot{h}_{GPS})^2}{\sum w_i}} \quad (5)$$

where the weight,

$$w_i = \frac{1}{\sigma_{GPS}^2 + \sigma_{GIA}^2} \quad (6)$$

incorporates both the uncertainty of the individual GPS stations (σ_{GPS}) as well as the uncertainty of the GIA estimate (σ_{GIA} , described later in Sect. 5.1) at the station location. The uncertainties for the GPS stations ranged from < 0.3 mm (indicated by large symbols in Fig. 11), 0.3 to 1.5 mm (medium symbols), and > 1.5 mm (small symbols). Additional details of the comparisons to the GPS displacements will be discussed later in Sect. 5.

4 GIA bias correction

One of the early observations from the combination results was the presence of a mm-level bias in the empirically derived GIA rates. Earlier investigations into this suggested that the cause of this bias could come from several sources (Gunter et al., 2010). For example, if there exists a secular trend in the geocenter motion (degree 1 coefficients), then any Z-component rate would be unaccounted for in this analysis. The uncertainty in the determination of $C_{2,0}$ (related to Earth's oblateness) from GRACE has been recognized for some time, and is why values from satellite laser ranging are still recommended to be used in place of those found in the official data products. Any trend

Estimation of present-day Antarctic GIA and ice mass change

B. C. Gunter et al.

Title Page

Abstract

Introduction

Conclusions

References

Tables

Figures

◀

▶

◀

▶

Back

Close

Full Screen / Esc

Printer-friendly Version

Interactive Discussion



Estimation of present-day Antarctic GIA and ice mass change

B. C. Gunter et al.

Title Page

Abstract

Introduction

Conclusions

References

Tables

Figures

⏪

⏩

◀

▶

Back

Close

Full Screen / Esc

Printer-friendly Version

Interactive Discussion



or other inconsistency in the coefficient values used for $C_{2,0}$ would translate into a rate bias for Antarctica. Errors in the ICESat campaign bias could also contribute to the differences seen, as would any inconsistency in reference frames used by the various data sets. It is important to note that every 1 mm of offset in the GIA rates would translate into approximately 50 Gtyr^{-1} of solid-earth mass change, so while the magnitude of the offset is small, its impact on the solution can be significant.

To address the issue of potential offsets in the solutions, use was made again of the LPZ shown in Fig. 5. The rate of GIA in this region is expected to be very small, i.e., significantly less than the unknown bias offset caused by the various sources discussed above. As such, the LPZ is used as a calibration area, where both the mean surface height change (Sect. 3.2.2) and subsequent GIA is assumed to be zero in that region. In terms of a practical implementation, this is accomplished by computing the mean value over the LPZ of the smoothed \dot{h}_{GIA} values generated from Eq. (3). This mean value, termed the “LPZ GIA bias”, is then removed from all GIA values uniformly. The magnitude of the LPZ GIA bias for each case investigated is shown in Table 2.

Calibrating the solutions to the LPZ provides a simple but effective way to deal with the range of bias contributors (i.e., geocenter, reference frame, campaign bias, etc.) that are currently not known at the mm-level or less. The LPZ bias correction also allows each solution to be compared more equivalently, since the bias contributors which are removed may be different for each case. The primary consequence for using the LPZ in this way is that the GIA solutions created become regional to Antarctica, and therefore cannot be used to estimate global GIA effects, such as the contributions from the Northern Hemisphere.

5 Combination results

The geographical plots of a select set of the resulting GIA models created from the LPZ calibration approach are shown in Fig. 9 (the full set of plots can be found in Fig. S2 of the Supplement). The corresponding mass change values are provided in Table 2, ex-

pressed in total gigatons per year (Gtyr^{-1}) and divided into regions representing East Antarctica (EA), West Antarctica (WA), and the total Antarctic Ice Sheet (AIS), following the grounding lines defined by Zwally et al. (2012) (extended outwards by 400 km to account for the smoothing). Once the GIA mass change rates were obtained, they were subtracted from the total mass change estimated from GRACE to derive a corresponding ice mass change value, also shown in Table 2. Since the earlier LPZ GIA bias was estimated using all components in Eq. (3) (i.e., including SMB, surface heights, and GRACE), in order to compute the ice mass change estimates in a consistent manner, a separate LPZ bias was estimated for only GRACE, i.e., the “LPZ GRACE bias”, the values of which are shown in Table 2 in units of EWH. Again, this is done to ensure that the mean value of mass change over the LPZ is set to zero.

5.1 Uncertainty analysis

Errors in the GIA and ice mass change estimates from the combination approach were computed using formal error propagation techniques, resulting in what are believed to be realistic error uncertainties. Where possible, uncertainties provided for the individual input sources were used, while for other sources certain assumptions were made, the details of which are outlined below.

For the GRACE data, the uncertainties were derived using formal error propagation techniques and the publicly available calibrated errors provided by the CSR for each monthly solution, along with the uncertainties provided with the degree 1 and $C_{2,0}$ coefficients. The calibrated errors were first propagated into equivalent water height (EWH) using the functional model described by Wahr et al. (1998). These errors were in turn propagated onto the trend component, using the same parameterization described earlier in Sect. 3.1. Though not shown, the GRACE errors do have a latitudinal dependency to them, but for Antarctica they are relatively uniform at approximately $1\text{--}1.5\text{ mm yr}^{-1}$ EWH. It is important to note that the errors for GRACE are assumed to be the same for all solutions evaluated, and which is a source of future refinement for the

Estimation of present-day Antarctic GIA and ice mass change

B. C. Gunter et al.

Title Page

Abstract

Introduction

Conclusions

References

Tables

Figures

⏪

⏩

◀

▶

Back

Close

Full Screen / Esc

Printer-friendly Version

Interactive Discussion

combination approach. The errors for the ICESat trends made use of the EVUW-scaled uncertainties discussed in Sect. 3.2, which are shown in Fig. 4b. The FDM provided has associated uncertainties, as shown in Fig. 7b; however, the SMB information used to determine \dot{m}_{firn} in Eq. (3) do not have estimated uncertainties, so a standard deviation of 10% of the value for each grid point was used as a conservative estimate, similar to that employed by Rignot et al. (2008). For the rock densities, a standard deviation representing 100 kg m^{-3} of the value for each grid point was assumed. Likewise, for the surface density value used when treating the differences between ICESat and the FDM, a 10% standard deviation was also used per grid point.

The aforementioned input data uncertainties were then formally propagated using Eq. (3) to generate total uncertainties for the three major mass change quantities (total mass change, GIA-related mass change, and ice mass change) for EA, WA, and the AIS. The uncertainties for the AIS were computed by taking the square-root of the sum-of-squares of the EA and WA uncertainties. This is consistent with the analysis done as part of the recent Ice Sheet Mass Balance Intercomparison Exercise (IMBIE) (Shepherd et al., 2012), and is justified by the fact that the primary signals in EA and WA are sufficiently separated that their errors can be treated as independent of each other. These results are summarized on the last row of Table 2, with the geographical variation of the uncertainties shown in Fig. 10. The GIA uncertainties ($1-\sigma$) over the AIS are 40 Gtyr^{-1} , with the regions of higher uncertainties located in the areas most expected, such as the Amundsen Sea Sector (ASE) and Wilkes/Adelie Land (WA). The ice mass change estimates are relatively well defined for WA at 22 Gtyr^{-1} , with more uncertainty over EA, due primarily to the much larger surface area involved. In general, the ice mass change uncertainties match those of the IMBIE study, as well as other recent studies (King et al., 2012; Jacob et al., 2012). The GIA uncertainty rates are inherently difficult to quantify with current modeling techniques, and is therefore one of the strengths of the data-driven approach. A more detailed discussion on the implications of these uncertainties on the results will be provided in the next sections.

Estimation of present-day Antarctic GIA and ice mass change

B. C. Gunter et al.

Title Page

Abstract

Introduction

Conclusions

References

Tables

Figures

⏪

⏩

◀

▶

Back

Close

Full Screen / Esc

Printer-friendly Version

Interactive Discussion



5.2 Comparisons with GPS ground stations

To gain more insight into the performance of the estimated GIA rates, as well as to ensure an equal comparison with existing GIA models, the GPS rates were compared to several variants of the estimated GIA uplift rates. The first approach uses the same WRMS calculation described by Eqs. (5) and (6), using the empirical rates corrected with the LPZ GIA bias described earlier, along with the estimated GPS and GIA uncertainties. Both the full 35-station set of GPS stations were used, as well as a smaller subset of 29 stations. The 29-station subset was chosen to remove the influence that stations on Graham Land (GRA) might have on the WRMS calculations, as well as two other stations which showed vertical rates with large differences ($> 5 \text{ mm yr}^{-1}$), or were opposite in sign, to neighbouring GPS sites. GRA is a particularly dynamic region, and there are many factors that could impact the comparison of the GPS and derived GIA rates (Scambos et al., 2004; Thomas et al., 2011). Examples include potentially strong elastic effects on the GPS stations, the fact that ICESat is relatively data poor in this region, and the ability of GRACE to resolve the mass change of narrow north–south oriented features. The WRMS comparisons for both sets of GPS stations are shown in Table 3, with the stations excluded in the 29-station subset designated by square symbols in Fig. 11.

The results shown in Table 3 are useful for evaluating the performance of the various individual cases computed from the combination approach, primarily because the uncertainty of the resulting GIA rates can be used in the WRMS calculation. For comparisons of the empirically derived GIA rates to those from existing GIA models, the uncertainties of these models are not always available. Therefore, the comparisons with the GIA models were handled slightly differently, with the intention of making the comparisons more equivalent. The individual assumptions and choice of Earth model parameters for each of the models is different, and again may result in a bias offset with the observed GPS rates. To account for these, a bias term was estimated and removed between the GPS and modelled-GIA rates before the WRMS was computed. A similar

Estimation of present-day Antarctic GIA and ice mass change

B. C. Gunter et al.

Title Page

Abstract

Introduction

Conclusions

References

Tables

Figures

⏪

⏩

◀

▶

Back

Close

Full Screen / Esc

Printer-friendly Version

Interactive Discussion



systematic bias term was also estimated for the empirical rates from the combination approach, and was removed in addition to the LPZ-bias term discussed previously. As shown in Table 4, the average systematic bias magnitude is approximately 1 mm yr^{-1} , and has an estimated uncertainty of $\sim 0.3 \text{ mm yr}^{-1}$, demonstrating the bias to be statistically significant. The removal of the GPS bias serves to reduce all solutions to the same frame as the GPS network, and ideally allows the WRMS values computed to reflect the spatial correlation with the station displacements and not additional systematic differences such as global reference frame differences or far-field model assumptions. In addition to the systematic bias correction, because model uncertainties are not provided for all models, only the uncertainties of the GPS stations were used in the WRMS calculations. This is equivalent to setting σ_{GIA} to zero in Eq. (6).

The empirical rates were compared to the rates predicted from three recent GIA models: the ICE-5G model (Peltier, 2004)¹, the IJ05 model (Ivins and James, 2005), and the W12a model (Whitehouse et al., 2012)². The Simon et al. (2010) revision of the IJ05 model was used (full sea-level equation and global ocean loading) with no Antarctic continent load change since 800 yr BP. Also included in the comparisons were the results from the earlier study by Riva et al. (2009) (Riva09). As before, comparisons were made using both the full 35 and 29-station data sets. The results are listed in Table 4, and show both the original WRMS and bias-corrected WRMS values. Note that the WRMS values shown for Riva09, IJ05 and ICE-5G are corrections to the values shown in Thomas et al. (2011), and partially repeated in Whitehouse et al. (2012), due to an error in their WRMS calculations (the updated values do not affect the ranking of these models in these earlier works). To visually examine the differences, a selection of three empirical solutions representing the various GRACE processing variations (CSR RL04 DDK5, CSR RL05 Reg, and DMT1-b) are plotted in Fig. 11 alongside the three GIA models, with all figures representing the 35-station case after adjustment for the

¹www.psmsl.org/train_and_info/geo_signals/gia/peltier/

²www.dur.ac.uk/pippa.whitehouse/

Estimation of present-day Antarctic GIA and ice mass change

B. C. Gunter et al.

Title Page

Abstract

Introduction

Conclusions

References

Tables

Figures

⏪

⏩

◀

▶

Back

Close

Full Screen / Esc

Printer-friendly Version

Interactive Discussion



study did not account for any surface height or density change caused by the sizeable amount of accumulation ($> 10 \text{ cm yr}^{-1}$, see Fig. 7) that takes place in the ASE, and assigned all volume loss a density of ice. Doing so generates a lower mass loss rate for the region; however, now that these surface processes are taken into account, the altimetry-derived mass loss is greater for the ASE, resulting in a positive mass offset when compared to GRACE that is interpreted as GIA uplift in the inversion.

Naturally, there are other plausible explanations for the observed uplift in the ASE. It is possible that the gridded ICESat height change maps may overestimate the total volume loss in the ASE, or that GRACE is underestimating the mass loss. In either of these cases, the unaccounted for positive mass differential would be interpreted as GIA uplift in the combination. Alternatively, the SMB estimates could be overestimating the amount of accumulation in the region, again causing the positive mass differential with what GRACE observes to be treated as GIA uplift. While no long-term GPS vertical rates are currently available in the ASE, there have been a handful of permanent stations recently installed which will help validate these claims³. These future GPS measurements should also help to clarify the magnitude and spatial extent of the uplift, as some of the GIA solutions predict more widespread uplift than others. In particular, the RL04-based solutions tend to produce a larger extent of GIA uplift over the ASE than the RL05-based solutions, while the RL05 solutions indicate more uplift over the FRIS.

In the Philippi/Denman (PD) sectors, the empirical GIA rates shows a stronger uplift pattern than those found in the GIA models (Figs. 9 and S3). It is not believed that the estimated uplift is the result of any unmodelled accumulation, as the ICESat and FDM results agree well in this region, and the positive mass anomaly in the area is consistently observed in the GRACE solutions (Fig. 2), in particular in the regularized solutions, which tend to have higher spatial resolution. Also, the uncertainty analysis does not suggest any unusual circumstances in the area. Unfortunately, the comparisons with the GPS rates are inconclusive, since the few stations in the area are located

³www.polenet.com

Estimation of present-day Antarctic GIA and ice mass change

B. C. Gunter et al.

Title Page

Abstract

Introduction

Conclusions

References

Tables

Figures



Back

Close

Full Screen / Esc

Printer-friendly Version

Interactive Discussion



on the perimeter of the region in question. As such, the presence of genuine GIA uplift in the region will require more investigation before this can be confirmed.

Looking at the WRMS values in Table 3, most solutions compare well with each other, with differences only at the $0.1\text{--}0.2\text{ mm yr}^{-1}$ level. Again, these were computed using only the LPZ GIA bias calibration and considering the uncertainty of both the GIA and GPS stations. When examining Table 4, which only considered GPS station uncertainties and removed an additional systematic bias term, more variation in the results can be seen. The CSR RL04 DDK3 solution showed the lowest WRMS after the systematic bias is removed at 1.1 mm yr^{-1} , but the results of the other regularized solutions for both RL04 and RL05 are comparable, particularly for the 35-station set. It is interesting to note that the RL04 solutions have a larger systematic bias correction than the RL05 solutions, which is likely due to the difference in reference frames used in the GPS and RL04 GRACE data processing. In nearly all cases, the 29-station results are lower than the 35-station set. When comparing the empirical results to the model results, either with or without the systematic bias removed, the empirical rates show consistently lower values, with the IJ05 model having the closest similarity in terms of WRMS and spatial distribution of GIA uplift.

Regarding the ice mass change estimates, the values for all cases were relatively consistent. This is primarily a consequence of the fact that the surface height change information was fixed to that determined by the altimetry and FDM. In the combination, this essentially determines the variability of the firn and ice layers, forcing any variation in mass change seen by GRACE to go into the GIA estimates. The empirically derived ice mass change rate of $-100 \pm 44\text{ Gtyr}^{-1}$ for the AIS from this study agrees to within a single standard deviation to the recent IMBIE study (Shepherd et al., 2012) for a similar time frame (-57 ± 50 , October 2003–December 2008, using W12a and IJ05_R2; $-137 \pm 49\text{ Gtyr}^{-1}$ using ICE-5G), and shows slightly more ice mass loss than the recent results by King et al. (2012) (-68.7 ± 17.5 , using W12a), but less ice loss than estimates by Jacob et al. (2012) (-165 ± 36 , $1-\sigma$, using ICE-5G). In particular, the increased GIA predicted for the ASE in this study produces significantly more ice

Estimation of present-day Antarctic GIA and ice mass change

B. C. Gunter et al.

Title Page

Abstract

Introduction

Conclusions

References

Tables

Figures

⏪

⏩

◀

▶

Back

Close

Full Screen / Esc

Printer-friendly Version

Interactive Discussion



uplift beneath the Ross and Filchner Ronne Ice Shelf. The empirical GIA rates generated from this approach showed good overall agreement to an independent set of GPS-derived vertical rates, although there are no long-term GPS records in some of the suspected uplift zones, such as the ASE and PD sectors, so the estimated vertical rates in these areas cannot currently be verified. Nonetheless, the results from the combination approach demonstrate that the technique has the potential to reduce the uncertainty surrounding both Antarctic GIA and ice mass change estimates.

Supplementary material related to this article is available online at:
<http://www.the-cryosphere-discuss.net/7/3497/2013/tcd-7-3497-2013-supplement.pdf>.

Acknowledgements. The authors would like to thank Pavel Ditmar and Hassan Hashemi Farahani for providing the DMT solutions, Himansu Save for the CSR Regularized solutions, and Jürgen Kusche for the DDK solutions. Additional thanks go to Pippa Whitehouse for the W12a GIA model, Erik Ivins for the IJ05 model, and Richard Peltier for the ICE-5G model. All figures were produced using the Generic Mapping Tools (GMT). This study was partially funded by the Division for Earth and Life Sciences (ALW) with financial aid from the New Netherlands Polar Programme (NNPP) of the Netherlands Organization for Scientific Research (NWO). MAK is a recipient of an Australian Research Council Future Fellowship (project number FT110100207).

References

- Chambers, D. P. and Bonin, J. A.: Evaluation of Release-05 GRACE time-variable gravity coefficients over the ocean, *Ocean Sci.*, 8, 859–868, doi:10.5194/os-8-859-2012, 2012. 3504
- Chen, J. L., Wilson, C. R., Blankenship, D. D., and Tapley, B. D.: Antarctic mass rates from GRACE, *Geophys. Res. Lett.*, 33, L11502, doi:10.1029/2006GL026369, 2006. 3498
- Cheng, M. and Tapley, B. D.: Variations in the Earth's oblateness during the past 28 years, *J. Geophys. Res.*, 109, B09402, doi:10.1029/2004JB003028, 2004. 3503

TCD

7, 3497–3541, 2013

Estimation of present-day Antarctic GIA and ice mass change

B. C. Gunter et al.

Title Page

Abstract

Introduction

Conclusions

References

Tables

Figures

⏪

⏩

◀

▶

Back

Close

Full Screen / Esc

Printer-friendly Version

Interactive Discussion



Estimation of present-day Antarctic GIA and ice mass change

B. C. Gunter et al.

Title Page

Abstract

Introduction

Conclusions

References

Tables

Figures

◀

▶

◀

▶

Back

Close

Full Screen / Esc

Printer-friendly Version

Interactive Discussion

- Ewert, H., Popov, S. V., Richter, A., Schwabe, J., Scheinert, M., and Dietrich, R.: Precise analysis of ICESat altimetry data and assessment of the hydrostatic equilibrium for sub-glacial Lake Vostok, East Antarctica, *Geophys. J. Int.*, 191, 557–568, doi:10.1111/j.1365-246X.2012.05649.x, 2012. 3508
- 5 Groh, A., Ewert, H., Scheinert, M., Fritsche, M., Rülke, A., Richter, A., Rosenau, R., and Dietrich, R.: An investigation of Glacial Isostatic Adjustment over the Amundsen Sea sector, West Antarctica, *Global Planet. Change*, 98–99, 45–53, doi:10.1016/j.gloplacha.2012.08.001, 2012. 3518
- Gunter, B., Urban, T., Riva, R., Helsen, M., Harpold, R., Poole, S., Nagel, P., Schutz, B., and Tapley, B.: A comparison of coincident GRACE and ICESat data over Antarctica, *J. Geodesy*, 83, 1051–1060, doi:10.1007/s00190-009-0323-4, 2009. 3499, 3507, 3508
- 10 Gunter, B., Riva, R., Urban, T., Harpold, R., Schutz, B., Nagel, P., and Helsen, M.: Evaluation of GRACE and ICESat mass change estimates over Antarctica, in: *Gravity, Geoid and Earth Observation*, edited by: Mertikas, S. P., vol. 135 of *International Association of Geodesy Symposia*, Springer, Berlin, Heidelberg, doi:10.1007/978-3-642-10634-7_75, 563–569, 2010. 3499, 3507, 3512
- 15 Horwath, M. and Dietrich, R.: Signal and error in mass change inferences from GRACE: the case of Antarctica, *Geophys. J. Int.*, 177, 849–864, doi:10.1111/j.1365-246X.2009.04139.x, 2009. 3498
- 20 Hughes, G. B. and Chraibi, M.: Calculating Ellipse Overlap Areas, available at: <http://arxiv.org/abs/1106.3787>, 2011. 3506
- Ivins, E. R. and James, T. S.: Antarctic glacial isostatic adjustment: a new assessment, *Antarct. Sci.*, 17, 541–553, 2005. 3517
- Jacob, T., Wahr, J., Pfeffer, W., and Swenson, S.: Recent contributions of glaciers and ice caps to sea level rise, *Nature*, 482, 514–518, 2012. 3498, 3515, 3520
- 25 Kaspers, K. A., van de Wal, R. S. W., van den Broeke, M. R., Schwander, J., van Lipzig, N. P. M., and Brenninkmeijer, C. A. M.: Model calculations of the age of firn air across the Antarctic continent, *Atmos. Chem. Phys.*, 4, 1365–1380, doi:10.5194/acp-4-1365-2004, 2004. 3510
- King, M. A., Bingham, R. J., Moore, P., Whitehouse, P. L., Bentley, M. J., and Milne, G. A.: Lower satellite-gravimetry estimates of Antarctic sea-level contribution, *Nature*, 491, 586–589, doi:10.1038/nature11621, 2012. 3515, 3520, 3521
- 30

Estimation of present-day Antarctic GIA and ice mass change

B. C. Gunter et al.

Title Page

Abstract

Introduction

Conclusions

References

Tables

Figures

◀

▶

◀

▶

Back

Close

Full Screen / Esc

Printer-friendly Version

Interactive Discussion

- Klees, R., Revtova, E. A., Gunter, B. C., Ditmar, P., Oudman, E., Winsemius, H. C., and Savenije, H. H. G.: The design of an optimal filter for monthly GRACE gravity models, *Geophys. J. Int.*, 175, 417–432, doi:10.1111/j.1365-246X.2008.03922.x, 2008. 3504
- 5 Kusche, J.: Approximate decorrelation and non-isotropic smoothing of time-variable GRACE-type gravity field models, *J. Geodesy*, 81, 733–749, doi:10.1007/s00190-007-0143-3, 2007. 3504
- Lenaerts, J. T. M., van den Broeke, M. R., van de Berg, W. J., van Meijgaard, E., and Kuipers Munneke, P.: A new, high-resolution surface mass balance map of Antarctica (1979–2010) based on regional atmospheric climate modeling, *Geophys. Res. Lett.*, 39, L04501, doi:10.1029/2011GL050713, 2012. 3509
- 10 Ligtenberg, S. R. M., Helsen, M. M., and van den Broeke, M. R.: An improved semi-empirical model for the densification of Antarctic firn, *The Cryosphere*, 5, 809–819, doi:10.5194/tc-5-809-2011, 2011. 3509
- Liu, X., Ditmar, P., Siemes, C., Slobbe, D., Revtova, E., Klees, R., Riva, R., and Zhao, Q.: DEOS Mass Transport model (DMT-1) based on GRACE satellite data: methodology, validation, and application to estimating the ice mass balance of Greenland, *Geophys. J. Int.*, 181, 769–788, 2010. 3503
- 15 Peltier, W.: Global glacial isostasy and the surface of the ice-age Earth: the ICE-5G (VM2) Model and GRACE, *Annu. Rev. Earth Planet. Sci.*, 32, 111–149, 2004. 3517
- 20 Rignot, E., Bamber, J., van den Broeke, M., Davis, C., Li, Y., van de Berg, W., and van Meijgaard, E.: Recent Antarctic ice mass loss from radar interferometry and regional climate modelling, *Nat. Geosci.*, 1, 106–110, doi:10.1038/ngeo102, 2008. 3498, 3511, 3515
- Riva, R. E. M., Gunter, B. C., Urban, T. J., Vermeersen, B. L. A., Lindenbergh, R. C., Helsen, M. M., Bamber, J. L., van den Broeke, M. R., and Schutz, B. E.: Glacial isostatic adjustment over Antarctica from combined ICESat and GRACE satellite data, *Earth Planet. Sc. Lett.*, 288, 516–523, doi:10.1016/j.epsl.2009.10.013, 2009. 3500, 3501, 3502, 3507, 3517, 3518, 3521
- 25 Save, H., Bettadpur, S., and Tapley, B.: Reducing errors in the GRACE gravity solutions using regularization, *J. Geodesy*, 86, 695–711, doi:10.1007/s00190-012-0548-5, 2012. 3504
- 30 Scambos, T. A., Bohlander, J. A., Shuman, C. A., and Skvarca, P.: Glacier acceleration and thinning after ice shelf collapse in the Larsen B embayment, Antarctica, *Geophys. Res. Lett.*, 31, L18402, doi:10.1029/2004GL020670, 2004. 3516

Estimation of present-day Antarctic GIA and ice mass change

B. C. Gunter et al.

Title Page

Abstract

Introduction

Conclusions

References

Tables

Figures

◀

▶

◀

▶

Back

Close

Full Screen / Esc

Printer-friendly Version

Interactive Discussion

- Seo, K.-W., Wilson, C. R., Chen, J., and Waliser, D. E.: GRACE's spatial aliasing error, *Geophys. J. Int.*, 172, 41–48, doi:10.1111/j.1365-246X.2007.03611.x, 2008. 3499, 3503
- Shepherd, A., Ivins, E. R., A, G., Barletta, V. R., Bentley, M. J., Bettadpur, S., Briggs, K. H., Bromwich, D. H., Forsberg, R., Galin, N., Horwath, M., Jacobs, S., Joughin, I., King, M. A., Lenaerts, J. T. M., Li, J., Ligtenberg, S. R. M., Luckman, A., Luthcke, S. B., McMillan, M., Meister, R., Milne, G., Mouginit, J., Muir, A., Nicolas, J. P., Paden, J., Payne, A. J., Pritchard, H., Rignot, E., Rott, H., Sørensen, L. S., Scambos, T. A., Scheuchl, B., Schrama, E. J. O., Smith, B., Sundal, A. V., van Angelen, J. H., van de Berg, W. J., van den Broeke, M. R., Vaughan, D. G., Velicogna, I., Wahr, J., Whitehouse, P. L., Wingham, D. J., Yi, D., Young, D., and Zwally, H. J.: A reconciled estimate of ice-sheet mass balance, *Science*, 338, 1183–1189, doi:10.1126/science.1228102, 2012. 3499, 3515, 3520
- Siegfried, M., Hawley, R., and Burkhart, J.: High-resolution ground-based GPS measurements show intercampaign bias in ICESat elevation data near summit, Greenland, *IEEE T. Geosci. Remote*, 49, 3393–3400, doi:10.1109/TGRS.2011.2127483, 2011. 3508
- Siemes, C., Ditmar, P., Riva, R., Slobbe, D., Liu, X., and Farahani, H.: Estimation of mass change trends in the Earth's system on the basis of GRACE satellite data, with application to Greenland, *J. Geodesy*, 87, 69–87, doi:10.1007/s00190-012-0580-5, 2013. 3503
- Simon, K., James, T., and Ivins, E.: Ocean loading effects on the prediction of Antarctic glacial isostatic uplift and gravity rates, *J. Geodesy*, 84, 305–317, doi:10.1007/s00190-010-0368-4, 2010. 3517
- Slobbe, D., Lindenbergh, R., and Ditmar, P.: Estimation of volume change rates of Greenland's ice sheet from ICESat data using overlapping footprints, *Remote Sens. Environ.*, 112, 4204–4213, doi:10.1016/j.rse.2008.07.004, 2008. 3500, 3505
- Swenson, S. and Wahr, J.: Post-processing removal of correlated errors in GRACE data, *J. Geophys. Res.*, 33, L08402, doi:10.1029/2005GL025285, 2006. 3504
- Swenson, S., Chambers, D., and Wahr, J.: Estimating geocenter variations from a combination of GRACE and Ocean Model output, *J. Geophys. Res.*, B08410, doi:10.1029/2007JB005338, 2008. 3503
- Thomas, I. D., King, M. A., Bentley, M. J., Whitehouse, P. L., Penna, N. T., Williams, S. D. P., Riva, R. E. M., Lavallee, D. A., Clarke, P. J., King, E. C., Hindmarsh, R. C. A., and Koivula, H.: Widespread low rates of Antarctic glacial isostatic adjustment revealed by GPS observations, *Geophys. Res. Lett.*, 38, L22302, doi:10.1029/2011GL049277, 2011. 3511, 3516, 3517

Estimation of present-day Antarctic GIA and ice mass change

B. C. Gunter et al.

Title Page

Abstract

Introduction

Conclusions

References

Tables

Figures

⏪

⏩

◀

▶

Back

Close

Full Screen / Esc

Printer-friendly Version

Interactive Discussion

- Thompson, P. F., Bettadpur, S. V., and Tapley, B. D.: Impact of short period, non-tidal, temporal mass variability on GRACE gravity estimates, *Geophys. Res. Lett.*, 31, L23S10, doi:10.1029/2003GL019285, 2004. 3499
- Urban, T. and Schutz, B. E.: ICESat sea level comparisons, *Geophys. Res. Lett.*, 32, L06619, doi:10.1029/2005GL024306, 2005. 3508
- Urban, T., Pie, N., Felikson, D., Gunter, B., Harpold, R., and Schutz, B.: Comparison of repeat track, crossover, and overlapping footprint elevation change methods from satellite altimetry: ICESat-1 elevation changes of Greenland and Antarctica, *Geophys. J. Int.*, in preparation, 2013. 3506, 3507
- Velicogna, I. and Wahr, J.: A method for separating Antarctic postglacial rebound and ice mass balance using future ICESat Geoscience Laser Altimeter System, Gravity Recovery and Climate Experiment, and GPS satellite data, *J. Geophys. Res.-Sol. Ea.*, 107, 2263, doi:10.1029/2001JB000708, 2002. 3500
- Velicogna, I. and Wahr, J.: Measurements of time-variable gravity show mass loss in Antarctica, *Science*, 311, 1754–1756, doi:10.1126/science.1123785, 2006. 3499
- Wahr, J., Molenaar, M., and Bryan, F.: Time variability of the Earth's gravity field: hydrological and oceanic effects and their possible detection using GRACE, *J. Geophys. Res.*, 103, 30205–30230, doi:10.1029/98JB02844, 1998. 3514
- Wahr, J., Wingham, D., and Bentley, C.: A method of combining ICESat and GRACE satellite data to constrain Antarctic mass balance, *J. Geophys. Res.*, 105, 16279–16294, 2000. 3499, 3500
- Whitehouse, P. L., Bentley, M. J., Milne, G. A., King, M. A., and Thomas, I. D.: A new glacial isostatic adjustment model for Antarctica: calibrated and tested using observations of relative sea-level change and present-day uplift rates, *Geophys. J. Int.*, 190, 1464–1482, doi:10.1111/j.1365-246X.2012.05557.x, 2012. 3512, 3517
- Zwally, J. H., Giovinetto, M. B., Beckley, M. A., and Saba, J. L.: Antarctic and Greenland Drainage Systems, GSFC Cryospheric Sciences Laboratory, available at: http://icesat4.gsfc.nasa.gov/cryo_data/ant_grn_drainage_systems.php, (last access: 12 July 2013), 2012. 3507, 3514

Estimation of present-day Antarctic GIA and ice mass change

B. C. Gunter et al.

Title Page

Abstract

Introduction

Conclusions

References

Tables

Figures

⏪

⏩

◀

▶

Back

Close

Full Screen / Esc

Printer-friendly Version

Interactive Discussion

Table 1. Estimated ICESat campaign biases and uncertainties by campaign.

Campaign	Start Date	End Date	#Days	Bias (m)	σ (m)
1a/b	20 Feb 2003	29 Mar 2003	38	−0.046	0.017
2a	25 Sep 2003	19 Nov 2003	55	−0.057	0.015
2b	17 Feb 2004	21 Mar 2004	34	−0.038	0.017
2c	18 May 2004	21 Jun 2004	35	−0.004	0.047
3a	3 Oct 2004	8 Nov 2004	37	−0.053	0.034
3b	17 Feb 2005	24 Mar 2005	36	−0.035	0.023
3c	20 May 2005	23 Jun 2005	35	−0.019	0.024
3d	21 Oct 2005	24 Nov 2005	35	0.008	0.020
3e	22 Feb 2006	28 Mar 2006	34	0.009	0.013
3f	24 May 2006	26 Jun 2006	33	−0.002	0.026
3g	25 Oct 2006	27 Nov 2006	34	0.020	0.014
3h	12 Mar 2007	14 Apr 2007	34	0.015	0.010
3i	2 Oct 2007	5 Nov 2007	37	0.012	0.014
3j	17 Feb 2008	21 Mar 2008	34	0.031	0.013
3k	4 Oct 2008	19 Oct 2008	16	0.043	0.029
2d	25 Nov 2008	17 Dec 2008	23	0.029	0.025
2e	9 Mar 2009	11 Apr 2009	34	0.045	0.056
2f	30 Sep 2009	11 Oct 2009	12	0.037	0.055

Estimation of present-day Antarctic GIA and ice mass change

B. C. Gunter et al.

Table 2. Estimates of the mass change components derived from the data-driven approach. Uncertainties are $1-\sigma$.

Solution	Max Sph. Harm. deg × ord	LPZ bias		Total Est. Mass Change			Ice mass change,					
		GIA mmyr ⁻¹	GRACE mmyr ⁻¹ EWH	from GRACE (Gtyr ⁻¹)			Estimated GIA (Gtyr ⁻¹)			GRACE – GIA (Gtyr ⁻¹)		
				EA	WA	AIS	EA	WA	AIS	EA	WA	AIS
CSR RL04	60	1.8	1.4	57	-71	-13	52	34	87	5	-105	-100
CSR RL04 DDK3	60	1.7	1.0	53	-66	-13	48	40	87	5	-105	-100
CSR RL05	60	1.9	1.7	42	-77	-35	37	28	65	5	-105	-100
CSR RL05 DDK5	60	1.9	1.7	42	-78	-36	37	27	64	5	-105	-100
CSR RL05 Reg	120	1.9	1.7	42	-78	-36	36	27	63	5	-105	-100
GFZ RL04	120	1.8	1.2	58	-61	-3	53	45	98	4	-106	-101
GFZ RL04 DDK3	120	1.6	0.6	58	-59	-1	53	46	100	5	-105	-101
GFZ RL05	90	2.2	2.5	36	-81	-45	31	23	54	5	-105	-99
GFZ RL05 DDK5	90	2.1	2.4	39	-85	-47	33	19	53	5	-104	-99
DMT-1b	60	1.6	0.6	40	-58	-18	34	47	81	6	-106	-99
IJ05							33	41	74			
ICE-5G							53	48	101			
W12a							5	46	51			
Riva09							59	33	92			
Est. Uncertainties				18	6	19	34	21	40	38	22	44

Estimation of present-day Antarctic GIA and ice mass change

B. C. Gunter et al.

Table 3. Comparison of estimated GIA rates with GPS vertical rates, using the uncertainties for the both the GPS and GIA uplift rates in the WRMS calculations.

Solution	WRMS	
	29 GPS station set mm yr ⁻¹	35 GPS station set mm yr ⁻¹
CSR RL04	1.9	2.1
CSR RL04 DDK3	1.9	2.1
CSR RL05	1.8	2.1
CSR RL05 DDK5	1.8	2.1
CSR RL05 Reg	1.8	2.1
GFZ RL04	2.0	2.1
GFZ RL04 DDK3	2.0	2.1
GFZ RL05	1.8	2.0
GFZ RL05 DDK5	1.8	2.1
DMT-1b	1.8	2.0

[Title Page](#)
[Abstract](#)
[Introduction](#)
[Conclusions](#)
[References](#)
[Tables](#)
[Figures](#)
[⏪](#)
[⏩](#)
[◀](#)
[▶](#)
[Back](#)
[Close](#)
[Full Screen / Esc](#)
[Printer-friendly Version](#)
[Interactive Discussion](#)

Estimation of present-day Antarctic GIA and ice mass change

B. C. Gunter et al.

Title Page

Abstract

Introduction

Conclusions

References

Tables

Figures

⏪

⏩

◀

▶

Back

Close

Full Screen / Esc

Printer-friendly Version

Interactive Discussion

Table 4. Comparison of estimated GIA rates with GPS vertical rates, using only uncertainties for the GPS uplift rates in the WRMS calculations.

Solution	29 GPS station set			35 GPS station set		
	WRMS	Systematic bias	bias-corr. WRMS	WRMS	Systematic bias	bias-corr. WRMS
CSR RL04	1.7	1.3	1.2	1.9	1.2	1.5
CSR RL04 DDK3	1.7	1.3	1.1	1.9	1.2	1.4
CSR RL05	1.6	0.9	1.4	1.8	0.8	1.6
CSR RL05 DDK5	1.6	0.9	1.3	1.8	0.8	1.6
CSR RL05 Reg	1.6	0.9	1.3	1.8	0.8	1.6
GFZ RL04	1.9	1.1	1.5	1.9	1.1	1.6
GFZ RL04 DDK3	1.8	1.4	1.2	1.9	1.3	1.4
GFZ RL05	1.6	0.6	1.4	1.7	0.5	1.6
GFZ RL05 DDK5	1.6	0.8	1.4	1.8	0.6	1.7
DMT-1b	1.6	0.9	1.4	1.8	0.8	1.6
IJ05	3.4	2.5	2.2	3.4	2.4	2.4
ICE-5G	3.0	1.2	2.8	3.0	1.1	2.8
W12a	2.2	1.4	1.7	2.3	1.3	1.8
Riva09	2.1	1.6	1.4	2.2	1.5	1.7

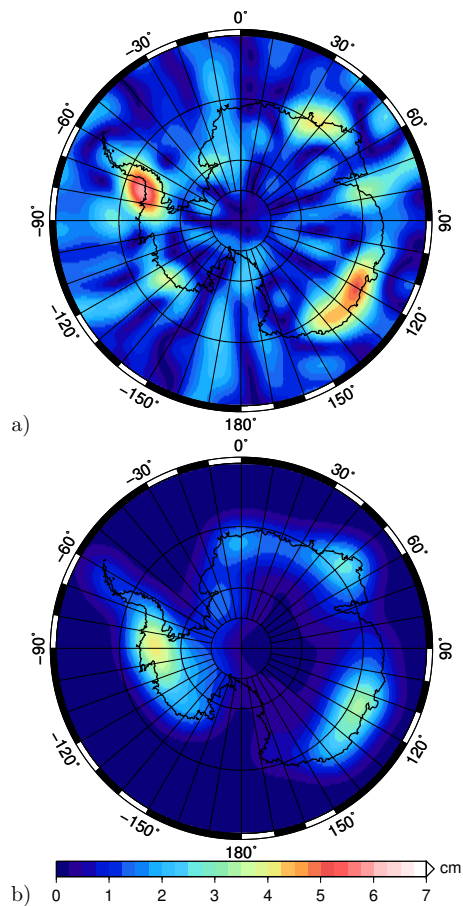


Fig. 1. Magnitude of K2-periodic signal in EWH for **(a)** GRACE CSR RL04 DDK3 and **(b)** RACMO2 SMB.

Estimation of present-day Antarctic GIA and ice mass change

B. C. Gunter et al.

Title Page

Abstract Introduction

Conclusions References

Tables Figures

◀ ▶

◀ ▶

Back Close

Full Screen / Esc

Printer-friendly Version

Interactive Discussion



Estimation of present-day Antarctic GIA and ice mass change

B. C. Gunter et al.

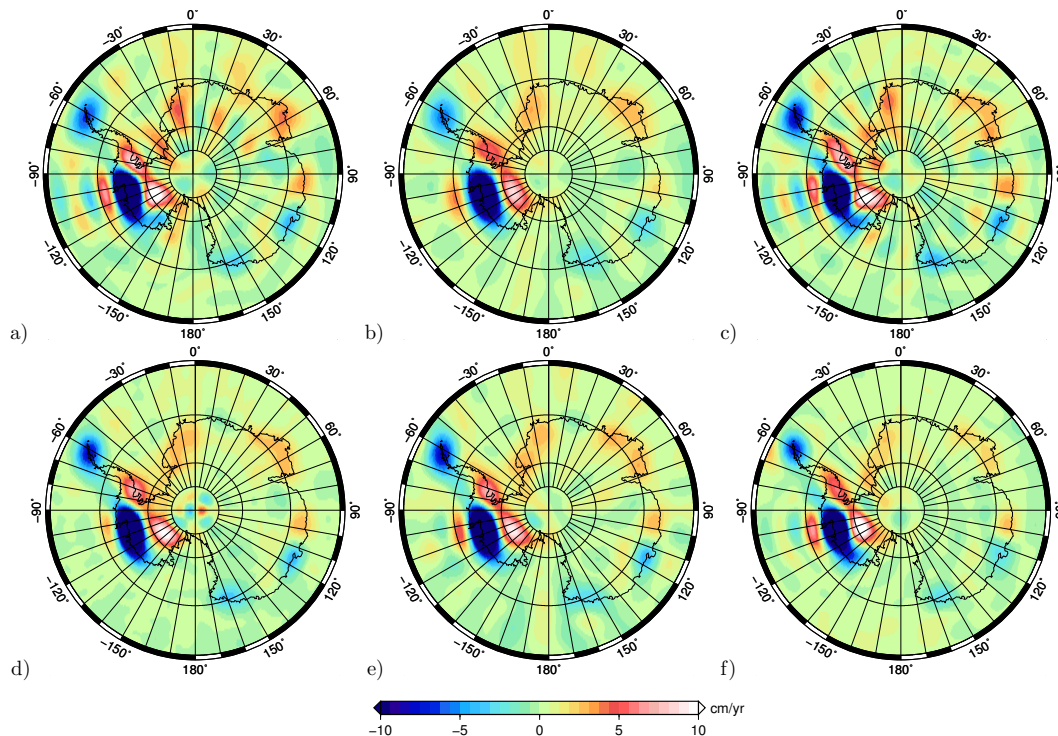


Fig. 2. Long-term mass change trends in units of EWH computed from the following GRACE solutions: **(a)** CSR RL04, **(b)** CSR RL04 DDK3, **(c)** CSR RL05, **(d)** CSR RL05 Regularized, **(e)** GFZ RL05 DDK5, **(f)** DMT-1b.

Estimation of present-day Antarctic GIA and ice mass change

B. C. Gunter et al.

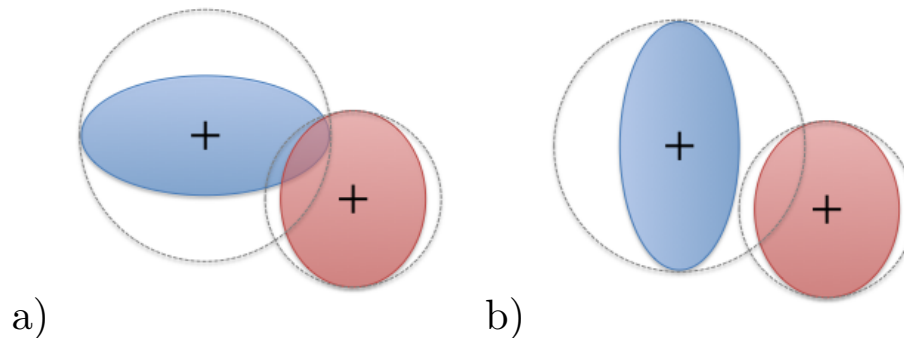


Fig. 3. Illustration of **(a)** an ICESat overlapping footprint (OFP) pair, and **(b)** near-neighboring shots.

[Title Page](#)[Abstract](#)[Introduction](#)[Conclusions](#)[References](#)[Tables](#)[Figures](#)[⏪](#)[⏩](#)[◀](#)[▶](#)[Back](#)[Close](#)[Full Screen / Esc](#)[Printer-friendly Version](#)[Interactive Discussion](#)

Estimation of present-day Antarctic GIA and ice mass change

B. C. Gunter et al.

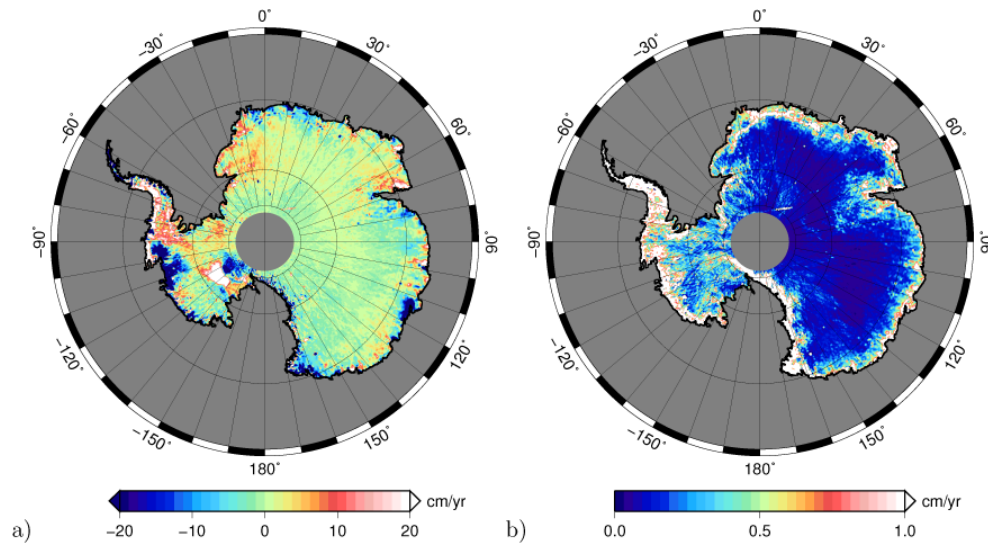


Fig. 4. (a) ICESat dh/dt estimates from the OFP approach and, (b) corresponding uncertainties.

[Title Page](#)[Abstract](#)[Introduction](#)[Conclusions](#)[References](#)[Tables](#)[Figures](#)[⏪](#)[⏩](#)[⏴](#)[⏵](#)[Back](#)[Close](#)[Full Screen / Esc](#)[Printer-friendly Version](#)[Interactive Discussion](#)

Estimation of present-day Antarctic GIA and ice mass change

B. C. Gunter et al.

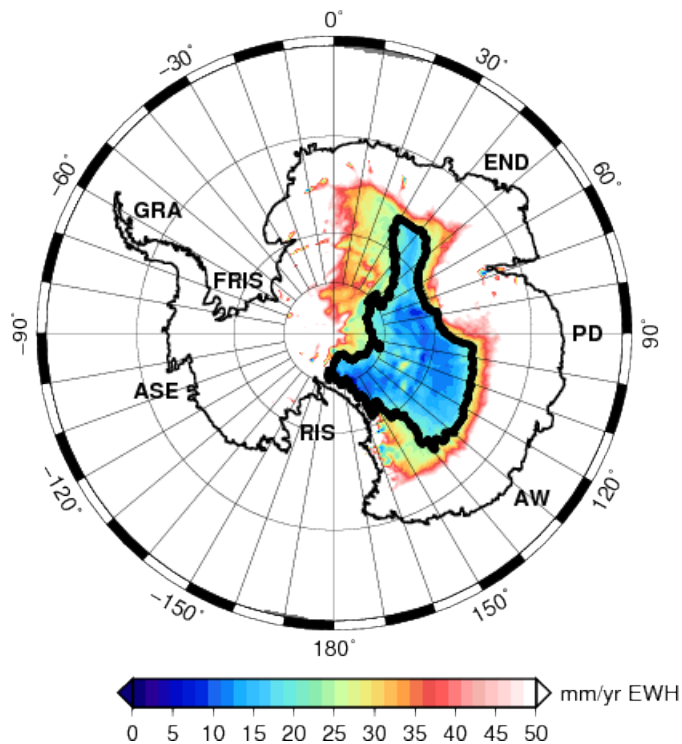


Fig. 5. Outline of the low-precipitation zone (LPZ) overlaid onto estimates of average yearly solid precipitative flux in units mmEWHyr^{-1} , together with the following location indicators: Amundsen Sea (ASE), Graham Land (GRA), Filchner Ronne Ice Shelf (FRIS), Enderby Land (END), Philippi/Denman (PD), Wilkes/Adelie Land (WA), Ross Ice Shelf (RIS).

Title Page

Abstract

Introduction

Conclusions

References

Tables

Figures

◀

▶

◀

▶

Back

Close

Full Screen / Esc

Printer-friendly Version

Interactive Discussion

Estimation of present-day Antarctic GIA and ice mass change

B. C. Gunter et al.

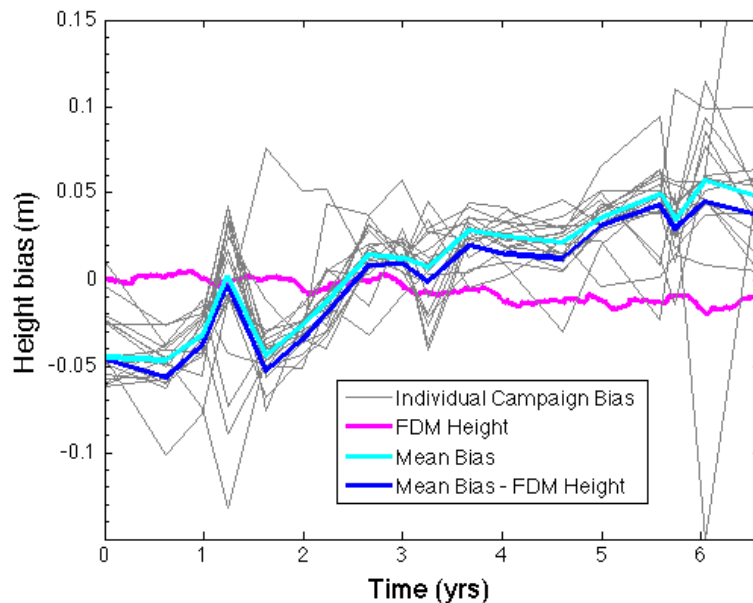


Fig. 6. Illustration of the ICESat campaign biases determined over the LPZ for each individual campaign (grey), the mean value (blue), and the mean minus the surface deformation (cyan) predicted from the FDM (magenta).

[Title Page](#)[Abstract](#)[Introduction](#)[Conclusions](#)[References](#)[Tables](#)[Figures](#)[⏪](#)[⏩](#)[◀](#)[▶](#)[Back](#)[Close](#)[Full Screen / Esc](#)[Printer-friendly Version](#)[Interactive Discussion](#)

Estimation of present-day Antarctic GIA and ice mass change

B. C. Gunter et al.

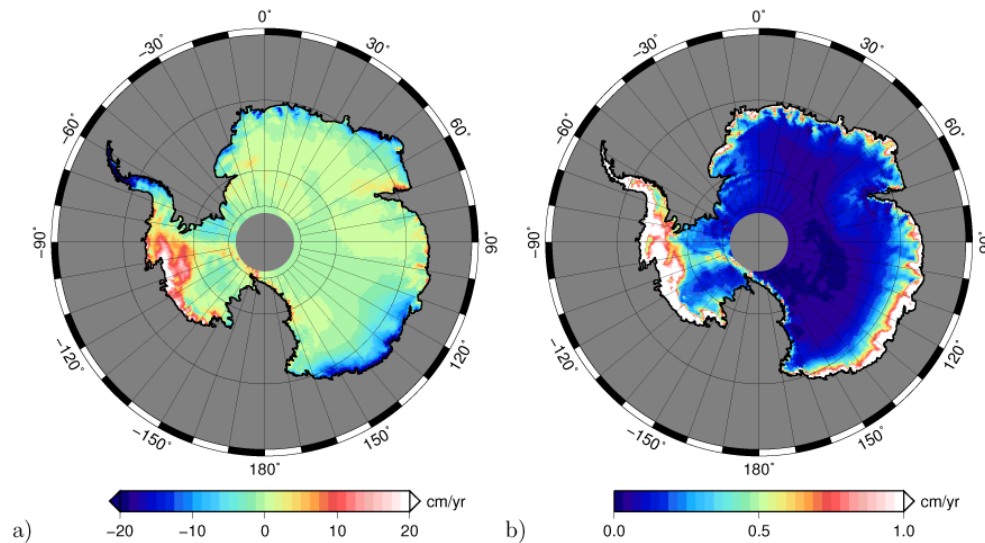


Fig. 7. (a) FDM surface height velocities and (b) corresponding uncertainties.

Title Page

Abstract

Introduction

Conclusions

References

Tables

Figures

⏪

⏩

◀

▶

Back

Close

Full Screen / Esc

Printer-friendly Version

Interactive Discussion

Estimation of present-day Antarctic GIA and ice mass change

B. C. Gunter et al.

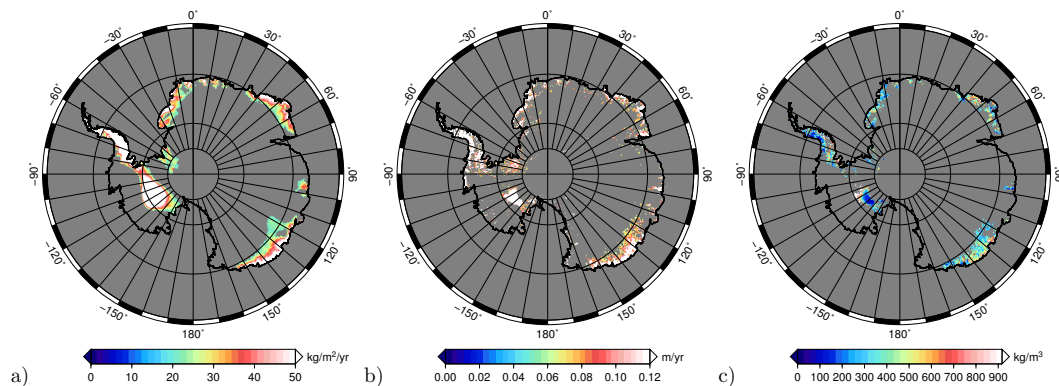


Fig. 8. (a) $(\text{GRACE} - \text{SMB}) > 20 \text{ kg m}^{-2} \text{ yr}^{-1}$, (b) $(\text{ICESat} - \text{FDM}) > 6 \text{ cm yr}^{-1}$, (c) Derived density (mean 396 kg m^{-3}).

Estimation of present-day Antarctic GIA and ice mass change

B. C. Gunter et al.

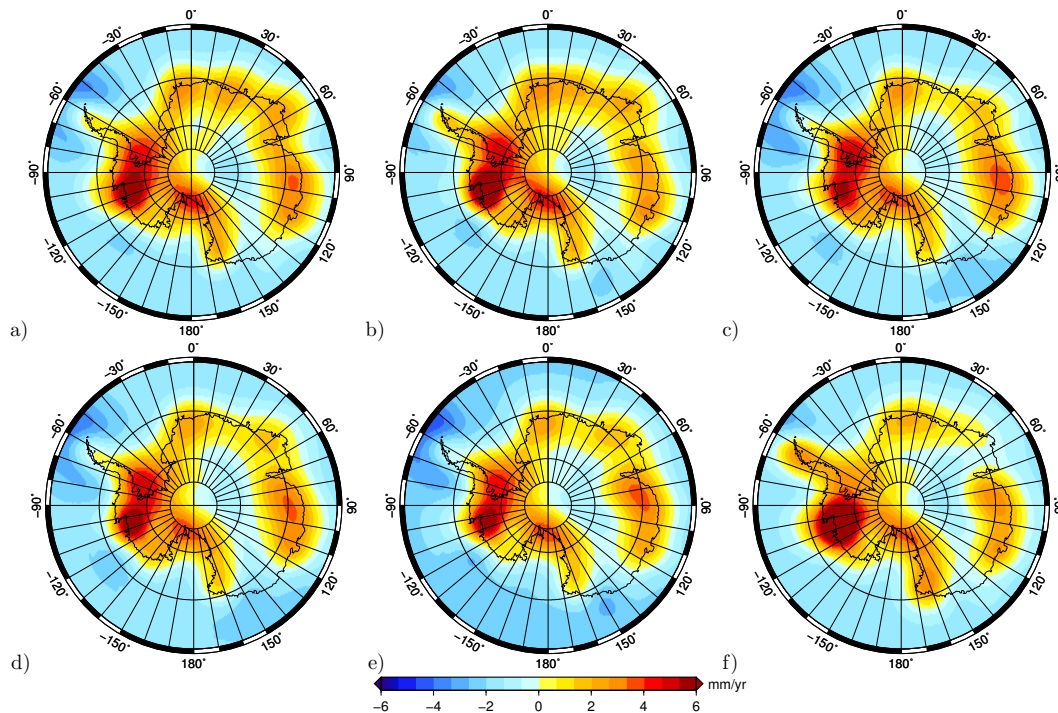


Fig. 9. Estimated GIA vertical rates computed from the following GRACE solutions: **(a)** CSR RL04, **(b)** CSR RL04 DDK3, **(c)** CSR RL05, **(d)** CSR RL05 Regularized, **(e)** GFZ RL05 DDK5, **(f)** DMT-1b.

Title Page

Abstract

Introduction

Conclusions

References

Tables

Figures

◀

▶

◀

▶

Back

Close

Full Screen / Esc

Printer-friendly Version

Interactive Discussion

Estimation of present-day Antarctic GIA and ice mass change

B. C. Gunter et al.

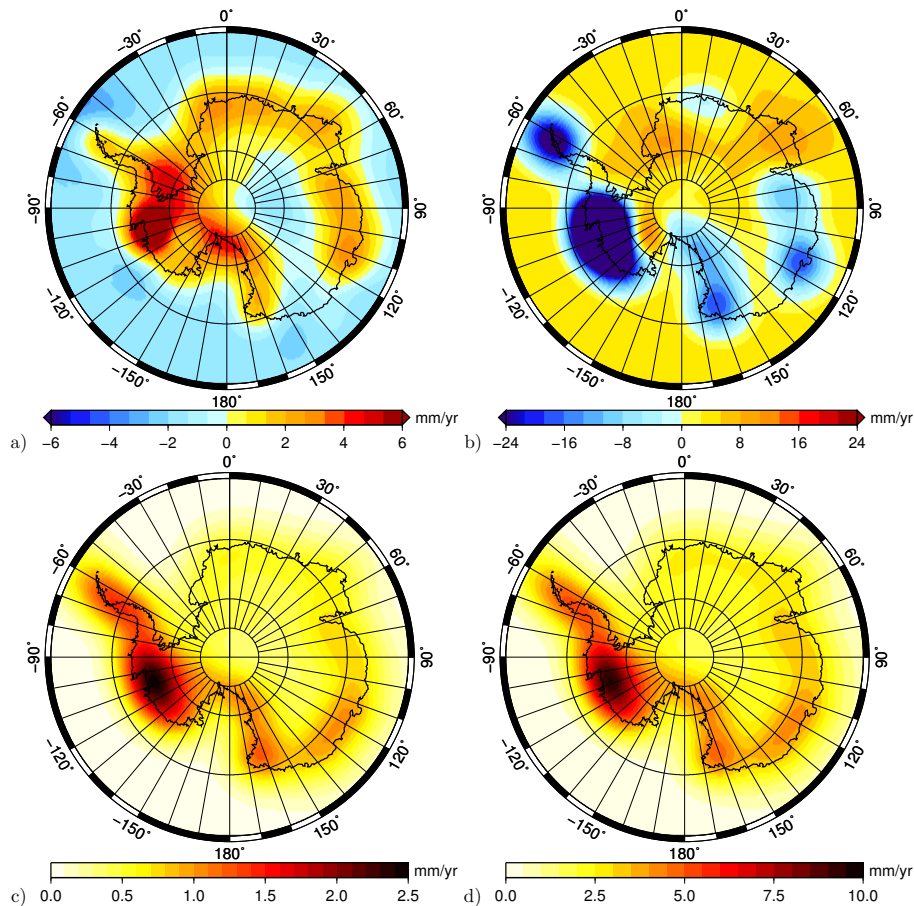


Fig. 10. Estimates (a, b) and uncertainties (c, d) for the empirically derived GIA rates (a, c) in mm yr^{-1} and ice mass change rates (b, d) in mm EWH yr^{-1} , using the representative case CSR RL04 DDK3.

Estimation of present-day Antarctic GIA and ice mass change

B. C. Gunter et al.

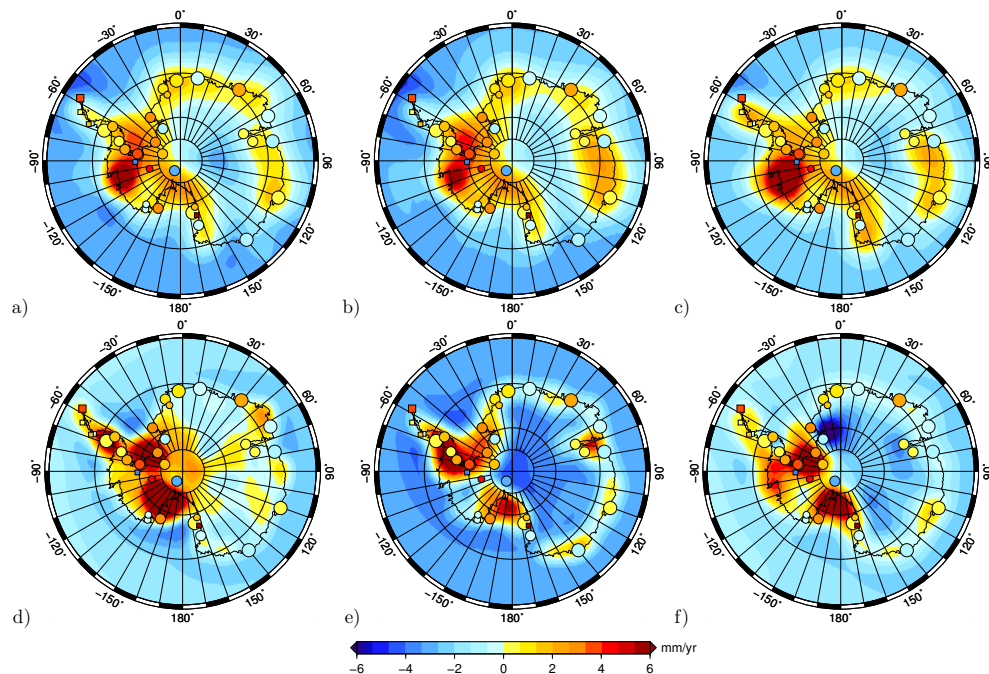


Fig. 11. Comparison of the 35-station WRMS, after an additional bias is removed with respect to the GPS rates, for **(a)** CSR RL04 DDK3, **(b)** CSR RL05 Reg, **(c)** DMT-1b, **(d)** ICE-5G, **(e)** IJ05, and **(f)** W12a.

Title Page

Abstract

Introduction

Conclusions

References

Tables

Figures

◀

▶

◀

▶

Back

Close

Full Screen / Esc

Printer-friendly Version

Interactive Discussion